

2017-02-01

The cold climate geomorphology of the Eastern Cape Drakensberg: A reevaluation of past climatic conditions during the last glacial cycle in Southern Africa

Mills, SC

<http://hdl.handle.net/10026.1/8086>

10.1016/j.geomorph.2016.11.011

Geomorphology

Elsevier BV

All content in PEARL is protected by copyright law. Author manuscripts are made available in accordance with publisher policies. Please cite only the published version using the details provided on the item record or document. In the absence of an open licence (e.g. Creative Commons), permissions for further reuse of content should be sought from the publisher or author.

**The cold climate geomorphology of the Eastern Cape Drakensberg:
A reevaluation of past climatic conditions during the last glacial
cycle in southern Africa**

S. C. Mills^{1*}, T. T. Barrows², M. W. Telfer¹, L. K. Fifield³

¹School of Geography, Earth and Environmental Sciences, Plymouth University,
Drake Circus, Plymouth, PL4 8AA, UK

²Department of Geography, University of Exeter, Exeter, Devon EX4 4RJ, UK

³Department of Nuclear Physics, Research School of Physics and Engineering,
Australian National University, Canberra, ACT 0200, Australia

*Corresponding author. Stephanie. C. Mills (stephanie.mills@plymouth.ac.uk)

Tel: (+44) (0)1752 585943.

**This manuscript is the final submitted version and contains errors that were
corrected during proofing. To access the published version, please see:
<http://www.journals.elsevier.com/geomorphology>**

Abstract

Southern Africa is located in a unique setting for investigating past cold climate geomorphology over glacial-interglacial timescales. It lies at the junction of three of the world's major oceans and is affected by subtropical and temperate circulation systems, therefore recording changes in Southern Hemisphere circulation patterns. Cold climate landforms are very sensitive to changes in climate and thus provide an opportunity to investigate past changes in this region. The proposed existence of glaciers in the high Eastern Cape Drakensberg mountains, together with possible rock glaciers, has led to the suggestion that temperatures in this region were as much as 10-17°C lower than present. Such large temperature depressions are inconsistent with many other palaeoclimatic proxies in southern Africa. This paper presents new field observations and cosmogenic nuclide exposure ages from putative cold climate landforms. We discuss alternative interpretations for the formation of the landforms and confirm that glaciers were absent in the Eastern Cape Drakensberg during the last glaciation. However, we find widespread evidence for periglacial activity down to an elevation of ~1700 m asl, as illustrated by extensive solifluction deposits, blockstreams, and stone garlands. These periglacial deposits suggest that the climate was significantly colder (~6°C) during the Last Glacial Maximum, in keeping with other climate proxy records from the region, but not cold enough to initiate or sustain glaciers or rock glaciers.

Keywords: Eastern Cape Drakensberg; surface exposure dating; periglacial geomorphology; palaeoclimate

1. Introduction

South Africa is positioned in a key location at the junction of three of the world's oceans and experiences a range of different climatic regimes owing to the influence of global circulation patterns and atmospheric processes. The magnitude of climate changes that occur in this region over glacial-interglacial cycles remains controversial, and the presence of glaciation in southern Africa during cold periods has attracted a wide range of research over a number of decades (e.g., Sparrow, 1967; Sanger, 1988; Marker, 1991; Grab, 1996, Lewis and Illgner, 2001; Mills and Grab, 2005; Mills et al., 2009a,b, 2012; Hall, 2010). Glacial and periglacial landforms are highly sensitive to temperature and precipitation and are excellent indicators of past climate change, provided they are correctly identified. Lewis and Illgner (2001) and Lewis (2008a) proposed that small glaciers could have existed at key sites in the high Eastern Cape Drakensberg mountains as a result of topographic shading and snowblow. However, the majority of recent work concerning past glaciation has been undertaken in Lesotho (Fig. 1), where Mills et al. (2012) proposed the occurrence of small-scale glaciation at much higher elevations. Glaciation in the Eastern Cape would require a climate 10–17°C colder than present (Lewis and Illgner, 2001) — a magnitude inconsistent with the reconstructed climate change in Lesotho.

In addition to proposed low elevation glaciation, a relict rock glacier has also been described from the Eastern Cape Drakensberg, suggesting the presence of permafrost at 1800 m asl (Lewis and Hanvey, 1993). However, Grab (2002) estimated that permafrost was only present above 3200 m asl in Lesotho. Contemporary periglacial conditions in the Eastern Cape Drakensberg are restricted to areas exceeding 2765 m asl (Kuck and Lewis, 2002), and it is assumed that the last time that extensive

periglacial and glacial conditions occurred is during the Last Glacial Maximum (LGM), which is defined as the period of maximum global ice volume (21 ± 2 ka; Mix et al., 2001). Climate proxy records for this period are relatively scarce for southern Africa because of the semi- and hyperarid climates not being conducive to the preservation of long-term palaeoenvironmental records (Chase, 2009). Those that do exist broadly suggest that temperatures were lower than present by 5-7°C (Heaton et al., 1986; Talma and Vogel, 1992; Holmgren et al., 2003), and a study in Lesotho using a glacier reconstruction and mass balance modelling approach suggested that glaciers could have existed there under these temperature reductions (Mills et al., 2012). Estimates of palaeoprecipitation are more problematic, and the climate of southern Africa has previously been considered as drier during the LGM (Partridge, 1997; Holmgren et al., 2003). However, more recent research has suggested that there may have been a shift in the rainfall zones allowing for increased precipitation in some areas during this time (Stuut et al., 2004; Chase and Meadows, 2007; Gasse et al., 2008; Brook et al., 2010; Mills et al., 2012; Scott et al., 2012). The extent of the shift of the rainfall zones is still poorly constrained by data, and a northward shift in the westerly wind belt would have increased the influence of the westerlies in the climate of South Africa (Chase and Meadows, 2007; Mills et al., 2012).

This paper aims to resolve the controversy regarding the extent of glaciation and cold climate processes in the Eastern Cape Drakensberg. We present the first surface exposure ages for cold climate landforms in southern Africa. Exposure dating provides a way of extending cold climate chronologies beyond glaciated landscapes (Barrows et al., 2004) and testing hypotheses of timing of formation. We also present new geomorphological and sedimentological observations of these landforms to determine

their mode of origin. Finally, this paper will present our findings within the context of the growing literature on late Pleistocene climates of southern Africa to better constrain past temperature changes.

2. Study area

The Eastern Cape Drakensberg mountains are situated close to the Lesotho border (Fig. 1), and the highest peak in this region is 3001 m asl at Ben Macdhui. The geology of the region is composed of Beaufort and Stormberg Group sandstones and argillaceous rocks with basaltic lavas of the Drakensberg Formation occurring at higher elevations. These basaltic lavas are interbedded with sandstones, pyroclastic rocks, tuffs, and agglomerates (Geological Survey, 1983). These largely flat-lying units exert a strong control on the topography of the region. Mean annual air temperature (MAAT) at 2788 m asl is ~7.5°C, although this is based on a limited record (1995/1996; Kück and Lewis, 2002). Freeze-thaw cycles are common at these elevations and occur on over 40% of days between May and September with an average of 63 frost days per annum (Kück and Lewis, 2002). The Eastern Cape Drakensberg falls within the summer precipitation zone of southern Africa, where over 66% of precipitation falls between April and September (Tyson and Preston-Whyte, 2000). Very few precipitation records exist and the WorldClim data set estimates precipitation at Ben Macdhui is ~940 mm/a (Hijmans et al., 2005).

2.1. Site descriptions

Putative glacial landforms were investigated at Mount Enterprise and Killmore along with a possible relict rock glacier in the Bottelnek Valley (Fig. 1). These sites were selected based on previous studies that described the presence of glacial or near

glacial conditions. A blockstream at Tiffendell was also investigated, and additional sites were examined at Carlisle's Hoek, along the Bokspruit, and at Moshesh's Ford to determine the lowest altitudinal limit of periglacial activity (Fig. 1).

Mount Enterprise reaches a maximum elevation of 2565 m asl, and the study site is located at 31.176° S, 27.980° E. Steep cliffs are located below the main peak, with their upper limits at ~2280 m asl. Ridges occurring between 2000 and 2100 m asl have been described by Lewis and Illgner (2001) as moraines (Fig. 2A). These ridges range from 120 to 250 m in length and are no more than 5 m in height. Lewis and Illgner (2001) undertook sedimentological analyses from within one of the ridges and a section, where they describe a diamicton, with the presence of clasts with occasional striations as indicative of glacial transport.

The Tiffindell area is located on a high plateau and hosts the highest peak in South Africa (Ben Macdhui) and the Tiffindell ski resort (Fig. 2B). The study area is located at 30.653° S, 27.937° E, and the region contains numerous periglacial deposits in the form of blockstreams, stone garlands, patterned ground, and gelifluction terraces. Kück and Lewis (2002) describe active gelifluction terraces occurring at altitudes between 2765 and 2855 m asl at Tiffindell. They measured temperature at ground level during the winter months and found that a diurnal range of over 10°C was not unusual (Kück and Lewis, 2002). Sorted polygons actively form at altitudes exceeding 2900 m asl on summit areas that are free of vegetation (Kück, 1996). The stone garlands and blockstreams are not presently active.

The Killmore site is located in the Bokspruit Valley (Fig. 1) at 30.948° S, 27.941° E and the highest peak is 2324 m asl. A 'bench' occurs on both sides of the valley at an elevation of ~2100 m asl and is formed by a concealed, more resistant layer of basalt (Geological Survey, 1983). Located on the bench on the western side of the valley is an accumulation of boulders that were initially described as a pronival rampart by Lewis (1994; Fig. 2C). This was later reinterpreted as a moraine ridge (Lewis, 2008b), based on the distance from the ridge crest to the backwall being greater than that proposed for pronival ramparts.

The Bottelnek region is an east-west trending valley drained by the Bottelnekspruit, with peaks reaching elevations >2300 m asl. Sediment accumulations occur along the walls of this valley, and Lewis and Hanvey (1993) suggested that some of these resembled relict rock glaciers. Organic material sampled from within one of the landforms described as a rock glacier in the Rose Hill area produced a radiocarbon date of 21,000 ± 400 ¹⁴C YBP, indicating that the sediment was deposited at or subsequent to this date (Lewis and Hanvey, 1993). The valley is composed of Clarens sandstone, with basalt occurring in the upper catchment and fluvial incision by the Bottelnekspruit exposing several sections through these units. We focus on the Rose Hill deposit located at 31.109° S, 27.777° E (Fig. 2D) that is proposed by Lewis and Hanvey (1993) to have the morphology (lobate / tongue-like feature) and sedimentology of a rock glacier.

Numerous periglacial deposits occur throughout the Eastern Cape Drakensberg, several of which have been described in detail by Lewis (2008b). Our study includes three additional locations where sections have been exposed in road cuttings at

Carlisle's Hoek (30.784° S, 27.970° E), Bokspruit (30.916° S, 27.920° E) and Moshesh's Ford (30.851° S, 27.781° E) (Fig. 1). The Carlisle's Hoek and Bokspruit sites are both underlain by Clarens sandstone, whereas Moshesh's Ford is a basaltic vent fill within the Clarens Formation (Lock et al., 1974).

3. Methods

Exposure dating was undertaken at suitable sites at Mount Enterprise and at Tiffindell; whilst the geomorphology was mapped at all sites, and the sedimentology of the deposits was described. At Mount Enterprise we targeted two ridges and a boulder terrace for surface exposure dating, collecting 11 samples in total. We sampled the largest boulders (most blocks sampled were 2-3 m long) along ridge crests to reduce the risk of exhumation through erosion. This site is backed by a high cliff, and therefore we consider risks associated with inheritance to be low. The blockstream at Tiffindell presented a challenge for exposure dating. The source area for blocks was restricted to low cliffs only a few metres high, 150 m above the deposit. Blocks have moved downslope to accumulate in the drainage line. Consequently, inheritance is more likely at this site, and ages are maximum ages for the formation of the deposit. We collected four samples in a longitudinal transect down the deposit to detect any age variations along its length.

The rock type at both sites was basalt, and so we chose to analyse the cosmogenic nuclide ^{36}Cl . Site information is presented in Table 1. The abundance of major target elements for ^{36}Cl production was determined using X-ray fluorescence. The concentrations of trace elements with large neutron capture cross sections (B, Gd, and Sm) and neutron-producing elements (U and Th) were measured by inductively

coupled plasma mass spectrometry. Chlorine content was determined by isotope dilution. The isotopic ratio of $^{36}\text{Cl}/\text{Cl}$ was measured by accelerator mass spectrometry on the 14UD accelerator at the Australian National University (Fifield et al., 2010). Chemical data are available on request.

Chlorine-36 exposure ages are calculated as detailed in Barrows et al. (2013). We calculated total production from spallation on K, Ca, Ti, and Fe and from muon capture on K and Ca, using the production rates of Stone et al. (1996a, 1996b, 1998), Evans (2001), and Masarik and Reedy (1995). For ^{36}Cl production by neutron capture on K and Cl, we followed the procedures of Liu et al. (1994), Phillips et al. (2001), and Stone et al. (1998) and calculated the nucleogenic contribution following Fabryka-Martin (1988). Production rates were scaled using the scheme of Stone (2000). All measurement errors, including production rate errors, are fully propagated on individual ages. No correction for weathering was applied. All ages are reported at one standard deviation.

4. Results

4.1. Mount Enterprise

The geomorphological map for this site is presented in Fig. 3. We identify two distinct vegetated linear ridges (A and B) between 2000 and 2100 m asl that have large basalt boulders up to 6 m in length on their surface. Ridge A is ~250 m in length, whilst ridge B is ~150 m in length. A further ridge (C) is located to the south where a road cut exposes a section (3). Boulder deposits (D and E) are located on a bench between 2100 and 2200 m asl. Talus slopes, boulder terraces, and landslide deposits also

occur in close proximity to the linear ridges, indicating that this area is geomorphologically active.

We present a sedimentological log of several exposed sections at this site in Fig. 4. Section 1 is ~10 m high and is not associated with a distinct ridge. This is the same section that Lewis and Illgner (2001) described as 'till'. The lower unit is ~6 m thick and is a massive matrix-supported diamicton with a fine interbed containing small clasts, dipping at ~35°. The clasts within the diamicton are subrounded to subangular and deeply weathered, usually with spheroidal onion skin weathering. The unit is crudely graded with much larger blocks in the lower parts of the unit, below the dipping interbed. The upper 3 m of the section is composed of alternating units of matrix-supported subangular to angular clasts, which are oriented downslope, and fine-grained layers of silty clay, which may reflect two buried palaeosols. A mixture of sandstone and basalt clasts occurs in all units.

Section 2 (Figs. 3 and 4) consists of a highly weathered lower unit with the presence of weathered core-stones, underlying an ~2-m-thick matrix-supported diamicton with clasts up to ~1 m in length. The lower unit correlates with section 1 and consists of a matrix-supported diamicton with blocks up to ~1.5 m in length. Many of the larger clasts have undergone onion skin weathering and have completely weathered in situ in some instances (Fig. 5). Weathering rinds are up to 12 cm in this lower unit. The upper unit is composed of angular clasts within a finer-grained matrix, and weathering rinds in this unit are <10 mm. The relatively high degree of weathering in the lower unit of the two sections in comparison to the upper unit is likely to represent great antiquity.

No sections dissect ridges A and B; however a section (3) is exposed through ridge C (Fig. 4). This section is ~2.5 m thick and is composed of ~1.25 m of highly weathered bedrock, with the presence of deeply weathered corestones, overlain by 1.0 m of matrix-supported diamicton. The diamicton unit is divided by a weakly developed palaeosol that is ~10 cm deep. Clasts within the diamicton range from a few centimetres to ~1.0 m and are predominantly angular to subangular. Ridge C is therefore bedrock-cored with a surficial layer of sediment.

The exposure ages obtained from ridges A and B and the boulder terrace are presented in Table 2. The bulk of the ages are much younger than the age previously suggested by Lewis and Illgner (2001) for these features. The two ridges and boulder terrace are distinctly separated in time without obvious evidence for inheritance. The boulder terrace was deposited between 5.0 ± 0.3 and 7.7 ± 0.4 ka, with an average age of 6.8 ± 1.5 ka ($X^2 = 22$). Below this feature, the upper ridge (A) has exposure ages between 9.2 ± 0.3 and 12.0 ± 0.7 ka with a mean age of 10.5 ± 1.2 ka ($X^2 = 3.7$). The lowest ridge (B) has two ages with a mean of 19.0 ± 2.1 ka ($X^2 = 3.6$). A third age (11.15 ± 0.58 ka) is similar in age to the upper ridge. This difference might be accounted for by the boulder rolling onto the lower ridge when the upper ridge was deposited.

4.2. Tiffindell

The slopes in this region are south-facing and are conducive to the preservation of late-lying snow as illustrated in the satellite image (Fig. 6A). The study site has numerous areas where bedrock outcrops, indicating a relatively thin regolith cover, and where moderately low cliffs occur in the upper part of the catchment. A

blockstream occurs between 2730 and 2785 m asl and is ~125 m in length and up to 15 m in width. The blocks that make up the blockstream are up to 2 m in length and show no preferred orientation. The blocks in the upper part of the blockstream are predominantly angular to subangular, becoming slightly more subrounded toward the lower areas. Ages obtained from blocks within the blockstream (Table 2) range from 12.7 ± 0.8 to 49.3 ± 2.5 ka. Samples were taken from the largest blocks with an unobstructed horizon in a transect along the blockstream. The two youngest ages overlap and have an average age of 13.1 ± 0.6 ka ($\chi^2 = 6.7$), which probably represents the time of stabilisation and suggests that the blockstream was active at the end of the Pleistocene. The scatter in the ages most likely reflects inheritance.

4.3. Killmore

A distinct ridge, ~500 m in length, is a prominent feature in the landscape below near vertical cliffs, which trend N-S (Fig. 7). The lithology here is vulnerable to physical weathering, and vertical cracks and column structures can be observed in the basalt cliff walls. The interbedded basaltic lavas in this area, which form layers of different strength characteristics, could also make this area prone to landsliding. Below these cliffs are vegetated fans and talus cones that occur along the length of the cliff. The ridge surface is subdued and almost flat toward its northern limits, and many large basalt boulders sit on and inside the ridge. A likely great age for these blocks is indicated by thick weathering rinds and some blocks are disintegrating in situ (e.g., Fig. 8), indicating that they are significantly older than those sampled from Mount Enterprise. Blocks making up the talus slopes inside the ridge are more angular and less weathered. Vesicles (usually infilled) occur as layers in the boulders and provide a 'way-up' criterion for determining the original orientation of the blocks. The dip and

strike of these layers was measured for 21 boulders in a boulder-rich, partly enclosed shallow depression of the ridge. In more than 75% of cases, the dip of the layers shows a significant orientation preference where the boulders have undergone rotation through $>75^\circ$, from vertical to nearly flat-lying (Fig. 7C); whereas the layers are also preferentially oriented in an easterly direction, which is perpendicular to the cliff face.

4.4. Rose Hill

The landform that we focus on in this area is located adjacent to Rose Hill farm (Fig. 9) and was previously interpreted as a rock glacier by Lewis and Hanvey (1993). The landform is not very distinct, although it has a lobate form in the lower part of the catchment that has been incised by fluvial activity. There is evidence of contemporary channel incision in the upper part of the catchment, most likely as a result of high-energy seasonal flow and snowmelt. In the lower parts of the catchment below ~2050 m asl, numerous locations with sandstone outcrops suggest that the regolith is locally thin. In August of 2011 a debris flow occurred, covering almost the entire lobate section of the 'rock glacier'. This debris flow accumulation spans an altitudinal range from 1950 to 2000 m asl and terminates as a series of 'fingers' that almost reach the river. The debris flow has a broad body up to 50 m across with boulders up to 1 m in diameter, intermixed with finer material. Clasts transported by the debris flow show linear impact / percussion marks, where clast collision has occurred during transport.

Fluvial incision by the Bottelnekspruit has exposed a section through the 'rock glacier' that is ~12 m high (Fig. 4). Bedrock comprised of Clarens sandstone forms the base of the section and is overlain by a diamicton composed of small, flat, angular clasts showing preferred orientation downslope, within a fine-grained matrix. The clasts in

this unit are sandstone, which suggests a local source from the bedrock. Overlying this unit is a diamicton with larger clasts and increasing amounts of basalt up profile, indicating increasing input from the upper catchment. Within the diamicton are intercalated, clast-supported alluvial units up to 10 cm in thickness, consisting of pebbles with very little fine matrix material. The upper unit is dominated by basalt and contains large clasts up to 2 m in length within a fine-grained matrix. A clast-supported bed is also present within this unit.

4.5. Periglacial deposits

The sections we studied at Carlisle's Hoek (1838 m asl) and Bokspruit (1844 m asl) are very similar and therefore we only present the section from Carlisle's Hoek (Fig. 4). Both sections are comprised of basal sandstone bedrock, overlain by a unit of flat clasts up to 15 cm in length, showing a strong preferred orientation in a southwesterly direction, which conforms to the direction of the slope. A silty unit underlies the present-day soil. At Moshesh's Ford (1740 m asl), there are alternating units of larger blocks (up to 30 cm) within a finer-grained matrix and finer sediments that are clast supported. Here the source material is columnar basalt, which has very small, thin columns and is more susceptible to fracturing. The clasts show no preferred orientation.

5. Discussion

5.1. Site interpretation

At Mount Enterprise we could find no direct evidence for glacial activity, and our observations indicate that an alternate model can explain the geomorphology in this

349 area. The site itself is not situated in a location that would be more conducive to
350 glaciation than other sites in this region. Areas of contemporary late-lying snow occur
351 preferentially on the higher south-facing slopes in this region, as observed in the field
352 and where depositional ridges are absent. The Mount Enterprise ridges superficially
353 resemble moraines but are not crescentic as expected for an ice source from the
354 direction of the cliffs. The lowermost ridge (B) and the ridge that has been exposed by
355 the road (C) are composed of sheets of diamicton that we propose are the result of
356 accumulation of colluvium through processes of landsliding and debris flows. The
357 diamicton sheets suggest various periods of enhanced mass movement activity and
358 multiple episodes of debris flow activity. The differences in weathering rind thickness
359 suggest that these processes have been ongoing for a substantial amount of time.
360 Subsurface weathering rinds of 4-10 cm in dolerite are known to be at least mid-
361 Pleistocene in age in a similar climate in Tasmania (Kiernan, 1990), which is similar to
362 those measured in the lower unit in sections 1 and 2 (Fig. 4). Debris flows are likely to
363 have been more frequent during the LGM when late-lying snow would have been more
364 extensive beneath the cliffs and when the ages obtained from the lower of the two
365 ridges (B) probably indicate mass movement during this time period. However, ridge
366 A and the boulder terrace were constructed about 10,000 years after the peak of the
367 LGM, during a warm climate interval. The landscape here has therefore been
368 generated by a series of rockfall, landslides, and debris flows, continuing to the present.
369 Although striated clasts have been described from this site (Lewis and Illgner, 2001),
370 these striae are not typical of glacial striae and match impact / percussion marks as
371 observed on the recent debris flow at Rose Hill, reflecting clast collision during
372 transport (Caballero et al., 2014). The burial of these clasts has allowed for the
373 preservation of these impact marks.

374

375 The Killmore site also only superficially resembles a glaciated site. The section
376 examined had a distinct ridge and a potential catchment for a small glacier / snow
377 patch under the steep cliffs. However, no evidence of former meltwater streams exists
378 and blocks show no evidence of transport by ice. Boulders are located on the proximal
379 side of the ridge, suggesting that they have originated from rockfall. The orientation of
380 these blocks perpendicular to the cliff face indicates that this feature most likely
381 represents a series of rotational landslides or topples. The heterogeneity of the site's
382 geology, comprised of different strength rocks such as basaltic lava, sandstone, tuff,
383 and agglomerate, would make this particular area prone to landsliding. Rockfalls are
384 among the most common type of slope movement in mountain regions worldwide
385 (Whalley, 1984; Flageollet and Weber, 1996) and the occurrence of numerous talus
386 slopes along the cliff face suggests that these processes are very active in this region.
387 Falls and topples occur where sufficiently steep slopes exist (van Beek et al., 2008),
388 and the near-vertical cliffs in some areas would make them conducive to such
389 processes. Vertical weaknesses in the bedrock create columns, such as those
390 observed on both sides of the valley at Killmore, which subsequently fail (Dikau et al.,
391 1996). Movement would have been arrested as a result of the width of the bench and
392 reduction in slope angle, allowing retention of the mass on the bench and creating
393 reverse slope back to the cliff. This area is at a significant altitude (>2000 m asl),
394 therefore freeze-thaw cycles could also have been important over long timescales for
395 weathering the rock prior to the occurrence of mass movement processes. The long-
396 term effect of climate in weakening the rock through weathering must be considered
397 as an important driving force of toppling processes (Dikau et al., 1996). Boulder

accumulations also occur on the bench on the opposite side of the valley, indicating that these processes are common in the region.

The Rose Hill site has a few features in common with rock glaciers, including its elongated profile and its thickness (Lewis and Hanvey, 1993). Rock glaciers are lobate or tongue-shaped landforms of frozen material (French, 2007), originating either as gradually creeping permafrost and ice-rich debris on nonglacierised slopes, or as debris-covered remnant glaciers in permafrost-free areas (Haeberli et al., 2006). They would therefore imply the presence of either permafrost or glacial ice. The Rose Hill landform has been interpreted as a relict rock glacier based on its morphology, stratigraphy, particle size, clast characteristics, and morphology of quartz grains (Lewis and Hanvey, 1993). A clear distinction between coarse debris overlying fine debris was identified, which commonly occurs in rock glaciers (Lewis and Hanvey, 1993). However, Zurawek (2003) suggested that this two-layered stratigraphy must be considered within a geomorphological context and that it should not be regarded as a prerequisite condition for the presence of a relict rock glacier. In fact, Zurawek (2003) stated that sedimentological properties are largely controlled by the source lithology and are of little value in identifying relict rock glaciers.

The rock glacier origin of the landforms found in the Bottelnekspruit region have recently been questioned by Grab (2000), who proposed that the morphology and sedimentology of some of the landforms may represent debris flow and solifluction processes. The Rose Hill landform has a number of features that indicate that it cannot be a rock glacier. Firstly, the lobate form contains several areas that are bedrock, exposed where the soil is thin. The overall topography of the western side of the

feature is governed by the underlying bedrock. Secondly, the internal structure of the Rose Hill feature does not clearly contain the two-layered stratigraphy proposed to be typical of a rock glacier. The lower sedimentary unit in the exposed face has a preferred orientation downvalley, indicative of solifluction processes (Nelson, 1985) acting upon locally derived sandstone, in the wrong direction for material originating from the catchment. The overlying unit is comprised of a series of debris flows with no clast-supported layer at the surface typical of rock glaciers. The interbedded alluvial units indicate that the sequence was accumulated sequentially and that the stream once flowed at a much higher base level during accretion. The upper parts of the catchment contain several avalanche couloirs, where snow likely accumulates under contemporary conditions. Greater snow accumulation during colder conditions and associated spring melt would enhance slope instability and increase the frequency of debris flows. Based on this evidence, we propose that the Rose Hill landform reflects an accumulation of sediment as a result of mass movement processes such as solifluction and debris flows over time with interbedded alluvial units.

The ages obtained from the blockstream at Tiffindell indicate that this was active during the last glaciation and ceased moving at the end of the Pleistocene. Tiffindell hosts the highest peak in South Africa, the slopes are south-facing, and this area retains the largest amount of late-lying snow in the region, yet glacial deposits are absent. The complete absence of glacial deposits, in possibly the most likely location in South Africa, is indirect evidence against glaciation at other less favourable sites such as Mount Enterprise. The extensive relict periglacial deposits as well as the dated blockstream, suggest that this was a periglacial environment during the late Pleistocene. Deep seasonal frost would have been necessary in order for mass

wasting processes associated with frost creep and block movement to take place. A similar deposit has been described by Boelhouwers et al. (2002) in the Lesotho Highlands at 3000-3200 m asl. This landform is much more extensive (>1 km in length) than those observed in the Eastern Cape, but it has also been attributed to the occurrence of deep seasonal frost and restricted snow cover during the LGM. The dated blockstream at Tiffindell has a slightly younger age than similar dated periglacial deposits in a similar climate in Australia (Barrows et al., 2004), where most periglacial activity occurred during the LGM.

5.2. Palaeoclimatic implications

Rock glaciers typically form in areas where the mean annual air temperature (MAAT) is $\leq -2^{\circ}\text{C}$ (Humlum, 1998). Therefore, Lewis (2008c) suggested that in order for rock glaciers to exist at 1800 m asl in the Eastern Cape Drakensberg, a temperature drop of $17\text{--}19^{\circ}\text{C}$ would be necessary during the LGM. In addition, for a glacier to have existed at Mount Enterprise, temperatures would have had to have been at least 10°C below present (Lewis and Illgner, 2001). The reevaluation of the cold-climate landforms in the Eastern Cape Drakensberg and the absence of evidence for glaciation has important implications for the palaeoclimate in this region. There is evidence that humans abandoned high altitude sites in this region from ~24 to 12 ka, most likely because of harsh climatic conditions (Lewis, 2008c). Climate data obtained from the South Africa weather bureau (Lewis and Illgner, 2001) indicates that at Rhodes (1676 m asl), MAAT is 11.8°C , and the coldest four-month average is 6.3°C . This suggests that a temperature depression of $6\text{--}7^{\circ}\text{C}$ would allow for the duration and cyclic pattern of ground temperatures passing below 0°C to be much more frequent at elevations above 1700 m asl, which is in accordance with proxy records suggesting a

5-7°C temperature depression during the LGM (Heaton et al., 1986; Talma and Vogel, 1992; Scott, 1999; Holmgren et al., 2003).

Our proposed temperature depression of 6-7°C for the Eastern Cape Drakensberg also agrees with the distribution of widespread slope deposits that have been described by Lewis (2008b). In fact, Lewis (2008c) suggested that these would have formed when temperatures were ~6°C below present. However, he proposed that these deposits would have formed subsequent to the colder conditions when the rock glaciers were active. In addition, findings from the adjacent Lesotho Highlands also suggest that temperatures would have been in the order of ~6°C colder during the LGM. The evidence of small-scale niche glaciers during the LGM in eastern Lesotho has been described by Mills and Grab (2005) and Mills et al. (2009a,b, 2012). Moraines have been identified based on morphological, sedimentological, and micromorphological evidence; and ages obtained using soil organic matter from within the moraines range from ~14 to 20.5 cal ka (Mills et al., 2009a). Mass balance modelling of the former glaciers (Mills et al., 2012) suggests that this region could have sustained small glaciers based on a 6°C temperature depression. If a 10-17°C temperature drop had occurred, as suggested by Lewis and Illgner (2001), then this would imply that much more extensive glaciation would have occurred in the Lesotho Highlands. In addition, the presence of a relict rock glacier at 1800 m asl in the Eastern Cape Drakensberg would imply that permafrost would have also occurred at higher elevations; however, evidence for Pleistocene permafrost (large sorted patterned ground) only exists at elevations exceeding 3450 m asl in Lesotho (Grab, 2002).

The 6-7°C temperature depression suggested for the Eastern Cape Drakensberg during the LGM is not only in keeping with temperature depressions suggested for the wider southern African region but also other areas in the Southern Hemisphere, such as Australia and South America. A temperature depression of 8-9°C has been suggested for the LGM over mainland Australia and about 6°C for Tasmania (Galloway, 1965; Williams et al., 2009), whilst modelling results for southern Patagonia agree with a 6°C temperature depression during the LGM (Kaplan et al., 2008).

6. Conclusion

We have reevaluated the cold climate landforms in the Eastern Cape Drakensberg, and we present cosmogenic nuclide exposure ages from these landforms in order to determine the timing for their emplacement and obtain a better understanding of the process of landscape development. We find that glaciers were absent in the Eastern Cape Drakensberg during the LGM. The ages obtained from Mount Enterprise suggest a complex landscape history, reflecting the accumulation of colluvium through processes of landsliding and debris flow, creating ridges. The ages obtained from the Tiffindell blockstream indicate emplacement during the late Pleistocene, when temperatures were cold enough to permit the development of deep seasonal ice. The reevaluation of the Mount Enterprise, Rose Hill, and Killmore sites — along with the evidence from Tiffindell and periglacial deposits at lower elevations — indicates that periglacial conditions prevailed during the LGM, with temperature depressions of ~6°C, allowing for enhanced periglacial activity and mass movement processes.

Acknowledgements

This work was funded by the Royal Geographical Society Peter Fleming Award, awarded jointly to SM and TB. We thank the department of Rural Development and Land Reform for the provision of the 2009 rectified 0.5 m aerial imagery, all the landowners who kindly allowed us access to their land, and Dave Walker from 'Walkerbouts Inn' and Wikus Roodt for the help they provided in tracking down the details of all the landowners. We would also like to thank Colin Lewis for valuable comments on a draft of the manuscript as well as Prof Jasper Knight and an anonymous reviewer.

References

- Barrows, T.T., Stone, J.O., Fifield, L. K., 2004. Exposure ages for Pleistocene periglacial deposits in Australia. *Quaternary Science Reviews* 23, 697-708.
- Barrows, T.T., Almond, P., Rose, R., Fifield, L.K., Mills, S.C., Tims, S.G. 2013. Late Pleistocene glacial stratigraphy of the Kumara-Moana region, West Coast of South Island, New Zealand. *Quaternary Science Reviews* 74, 139-159.
- Boelhouwers, J.C., Holness, S., Meiklejohn, K.I., Sumner, P. D., 2002. Observations on a blockstream in the vicinity of Sani Pass, Lesotho highlands, southern Africa. *Permafrost and Periglacial Processes* 13, 251-257.
- Brook, G.A., Scott, L., Railsback, L.B., Goddard, E.A., 2010. A 35 ka pollen and isotope record of environmental change along the southern margin of the Kalahari from a stalagmite and animal dung deposits in Wonderwerk Cave, South Africa. *Journal of Arid Environments* 74, 870-884.

544 Caballero, L., Sarocchi, D., Soto, E., Borselli, L., 2014. Rheological changes induced
 545 by clast fragmentation in debris flows. *Journal of Geophysical Research: Earth*
 546 *Surface*. 119, 1800-1817.

547 Chase, B. M., 2009. Evaluating the use of dune sediments as a proxy for palaeo-
 548 aridity: A southern African case study. *Earth Science Reviews*. 93, 31-45.

549 Chase, B.M., Meadows, M.E., 2007. Late Quaternary dynamics of southern Africa's
 550 winter rainfall zone. *Earth Science Reviews* 84, 103-138.

551 Dikau, R., Schrott, L., Dehn, M., 1996. Topple. In: Dikau, R., Brunsden, D., Schrott,
 552 L. and Ibsen, M-L. (Eds). *Landslide recognition: Identification, movement and*
 553 *causes*. John Wiley & Sons Ltd. Chichester. 29-41.

554 Evans, J.M., 2001. Calibration of the production rates of cosmogenic ^{36}Cl from
 555 potassium. PhD thesis, The Australian National University, Canberra.

556 Fabryka-Martin, J.T., 1988. Production of radionuclides in the Earth and their
 557 hydrogeologic significance, with emphasis on chlorine-36 and iodine-129.
 558 Unpublished PhD thesis, The University of Arizona.

559 Fifield, L.K., Tims, S.G., Fujioka, T., Hoo, W.T., Everett, S.E., 2010. Accelerator
 560 mass spectrometry with the 14UD accelerator at the Australian National University.
 561 *Nuclear Instruments and Methods in Physics Research Section B: Beam Interactions*
 562 *with Materials and Atoms* 268, 858-862.

563 Flageollet, J. C., Weber, D., 1996. Fall. In: Dikau, R., Brunsden, D., Schrott, L.,
 564 Ibsen, M. L. (Eds.). *Landslide recognition*. John Wiley and Sons Ltd, Chichester.

565 French, H. M., 2007. The periglacial environment. John Wiley and Sons Ltd,
 566 Chichester.

567 Galloway, R.W., 1965. Late Quaternary Climates in Australia. The Journal of
 568 Geology 73, 603-618.

569 Gasse, F., Chalieu, F., Vincens, A., Williams, M.A.J., Williamson, D., 2008. Climatic
 570 patterns in equatorial and southern Africa from 30,000 to 10,000 years ago
 571 reconstructed from terrestrial and near-shore proxy data. Quaternary Science
 572 Reviews 27, 2316-2340.

573 Geological Survey., 1983. 1:250,000 geological series, 3026 Aliwal North.
 574 Department of Mineral and Energy Affairs, Pretoria.

575 Grab, S.W., 1996. Debris deposits in the high Drakensberg, South Africa: Possible
 576 indicators for plateau, niche and cirque glaciation. Zeitschrift für Geomorphologie,
 577 Supplementbände 103, 389-403.

578 Grab, S.W., 2000. Periglacial features. In: Partridge, T.C., Maud, R.R. (Eds). *The*
 579 *Cenozoic of southern Africa*. Oxford University Press, Oxford. 207-217.

580 Grab S.W., 2002. Characteristics and palaeoenvironmental significance of relict sorted
 581 patterned ground, Drakensberg plateau, southern Africa. Quaternary Science
 582 Reviews 21, 1729-1744.

583 Haeberli, W., Hallet, B., Arenson, L., Elconin, R., Humlum, O., Kääb, A., Kaufmann,
 584 V., Ladanyi, B., Matsuoka, N., Springham, S., Vonder Mühll, D., 2006. Permafrost
 585 creep and rock glacier dynamics. Permafrost and periglacial processes 17, 189-214.

586 Hall, K., 2010. The shape of glacial valleys and implications for southern African
587 glaciation. *South African Geographical Journal* 92, 35-44.

588 Heaton, T.H.E., Talma, A.S., Vogel, J.C., 1986. Dissolved gas palaeotemperatures
589 and ^{18}O variations derived from groundwater near Uitenhage, South Africa.
590 *Quaternary Research* 56, 79-88.

591 Hijmans, R.J., Cameron, S.E., Parra, J.L., Jones, P.G., Jarvis, A., 2005. Very high
592 resolution interpolated climate surfaces for global land areas. *International Journal of*
593 *Climatology* 25, 1965-1978.

594 Holmgren, K., Lee-Thorp, J.A., Cooper, G.R.J., Lundblad, K., Partridge, T.C., Scott,
595 L., Sithaldeen, R., Talma, A.S., Tyson, P.D., 2003. Persistent millennial-scale
596 climatic variability over the past 25,000 years in Southern Africa. *Quaternary Science*
597 *Reviews* 22, 2311-2326.

598 Humlum, O., 1998. The climatic significance of rock glaciers. *Permafrost and*
599 *periglacial processes* 9, 375-395.

600 Kaplan, M.R., Fogwill, C.J., Sugden, D.E., Hulton, N.R.J., Kubik, P. W., Freeman,
601 S.P.H.T., 2008. Southern Patagonian glacial chronology for the Last Glacial period
602 and implications for Southern Ocean climate. *Quaternary Science Reviews* 27, 284-
603 294.

604 Kiernan, K., 1990. Weathering as an indicator of the age of Quaternary glacial
605 deposits in Tasmania. *Australian Geographer* 21, 1-17.

606 Kück, K.M., 1996. Periglacial features in the vicinity of Tiffindell Ski Resort, north–
 607 east Cape Drakensberg, South Africa, and their implications for the development of
 608 the resort. Unpublished M. Sc. thesis, Rhodes University, Grahamstown.

609 Kück, K.M., Lewis, C.A., 2002. Terracettes and active gelifluction terraces in the
 610 Drakensberg of the Province of the Eastern Cape, South Africa: a process study.
 611 South African Geographical Journal 84, 214–225.

612 Lewis, C.A., 1994. Protalus ramparts and the altitude of the local equilibrium line
 613 altitude during the Last Glacial Stage in Bokspruit, East Cape Drakensberg, South
 614 Africa. Geografiska Annaler 76A, 37-48.

615 Lewis, C.A., 2008a. Glaciations and Glacial Features. In: Lewis, C.A. (ed).
 616 *Geomorphology of the Eastern Cape: South Africa*. NISC, Grahamstown. 127-148.

617 Lewis, C.A., 2008b. Periglacial features. In: Lewis, C.A. (ed). *Geomorphology of the*
 618 *Eastern Cape: South Africa*. NISC, Grahamstown. 149-185.

619 Lewis C.A., 2008c. Late Quaternary climatic changes, and associated human
 620 responses, during the last ~45000 yr in the Eastern and adjoining Western Cape,
 621 South Africa. Earth Science Reviews 88, 167-187.

622 Lewis, C.A., Hanvey, P.M. 1993. The remains of rock glaciers in Bottelnek, East Cape
 623 Drakensberg, South Africa. Transactions of the Royal Society of South Africa 48, 265-
 624 289.

625 Lewis C.A., Illgner P.M. 2001. Late Quaternary glaciation in Southern Africa: Moraine
 626 ridges and glacial deposits at Mount Enterprise in the Drakensberg of the Eastern
 627 Cape Province, South Africa. Journal of Quaternary Science 16, 365-374.

628 Liu, B., Phillips, F.M., Fabryka-Martin, J.T., Fowler, M.M., Stone, W.D., 1994.
629 Cosmogenic ^{36}Cl accumulation in unstable landforms 1. Effects of the thermal neutron
630 distribution. *Water Resources Research* 30, 3115-3125.

631 Lock, B.E., Paverd, A.L., Broderick, T.J. 1974. Stratigraphy of the Karoo volcanic rocks
632 of the Barkly East district. *Transactions of the Geological Society of South Africa* 77,
633 117-129.

634 Marker, M.E., 1991. The evidence for cirque glaciation in Lesotho. *Permafrost &*
635 *Periglacial Processes* 2, 21-30.

636 Masarik, J., Reedy, R.C., 1995. Terrestrial cosmogenic-nuclide production
637 systematics calculated from numerical simulations. *Earth and Planetary Science*
638 *Letters* 136, 381-395.

639 Mills, S.C., Grab, S.W., 2005. Debris ridges along the southern Drakensberg
640 escarpment as evidence for Quaternary glaciation in southern Africa. *Quaternary*
641 *International* 129, 61-73.

642 Mills, S.C., Grab, S.W., Carr, S.J., 2009a. Late Quaternary moraines along the
643 Sekhokong range, eastern Lesotho: Contrasting the geomorphic history of north- and
644 south-facing slopes. *Geografiska Annaler* 91A, 121-140.

645 Mills, S.C., Grab, S.W., Carr, S.J., 2009b. Recognition and palaeoclimatic
646 implications of late Quaternary niche glaciation in eastern Lesotho. *Journal of*
647 *Quaternary Science* 24, 647-663.

648 Mills, S.C., Grab, S.W., Rea, B.R., Carr, S.J., Farrow, A., 2012. Shifting westerlies
649 and precipitation patterns during the Late Pleistocene in southern Africa determined

650 using glacier reconstruction and mass balance modelling. *Quaternary Science*
 651 *Reviews* 55, 145–159.

652 Mix, A.C., Bard, E., Schneider, R., 2001. Environmental processes of the ice age:
 653 land, oceans, glaciers (EPILOG). *Quaternary Science Reviews* 20, 627-657.

654 Nelson, F. E., 1985. A preliminary investigation of solifluction macrofabrics. *Catena* 12,
 655 23-33.

656 Partridge, T.C., 1997. Cainozoic environmental change in southern Africa, with special
 657 emphasis on the last 200 000 years. *Progress in Physical Geography*. **21**. pp. 2-32.

658 Phillips, F.M., Stone, W.D., Fabryka-Martin, J.T., 2001. An improved approach to
 659 calculating low-energy cosmic-ray neutron fluxes near the land/atmosphere interface.
 660 *Chemical Geology* 175, 689-701.

661 Sängner, H., 1988. Recent periglacial morphodynamics and Pleistocene glaciations of
 662 the Western Cape folded belt, South Africa. In *Geomorphological Studies in Southern*
 663 *Africa*, Dardis, G.F, Moon, B.P. (Eds.), Balkema: Rotterdam, 383-388.

664 Scott, L., 1999. Vegetation history and climate in the Savanna biome south Africa
 665 since 190,000 ka: a comparison of pollen data from the Tswaing crater (the Pretoria
 666 Saltpan) and Wonderkrater. *Quaternary International* 57-58, 215-223.

667 Scott, L., Neumann, F.H., Brook, G.A., Bousman, C.B., Norstrom, E., Metwally, A.A.,
 668 2012. Terrestrial fossil-pollen evidence of climate change during the last 26 thousand
 669 years in Southern Africa. *Quaternary Science Reviews* 32, 100-118.

670 Sparrow, G.W.A., 1967. Southern African cirques and arêtes. *Journal of Geography*
 671 2, 9-11.

672 Stone, J.O., 2000. Air pressure and cosmogenic isotope production. Journal of
673 Geophysical Research 105, 23,753-23,759.

674 Stone, J.O., Allan, G.L., Fifield, L.K., Cresswell, R.G., 1996a. Cosmogenic chlorine-36
675 from calcium spallation. Geochimica et Cosmochimica Acta 60, 679-692.

676 Stone, J.O., Evans, J.M., Fifield, L.K., Cresswell, R.G., Allan, G.L., 1996b.
677 Cosmogenic chlorine-36 production rates from potassium and calcium. Radiocarbon
678 38, 170-171.

679 Stone, J.O.H., Evans, J.M., Fifield, L.K., Allan, G.L., Cresswell, R.G., 1998.
680 Cosmogenic chlorine-36 production in calcite by muons. Geochimica et
681 Cosmochimica Acta 62, 433-454.

682 Stuut, J.B.W., Crosta, X., van der Borg, K., Schneider, R., 2004. Relationship
683 between Antarctic sea ice and southwest African climate during the late Quaternary.
684 Geology 32, 909-912.

685 Talma, A.S., Vogel, J.C., 1992. Late Quaternary paleotemperatures derived from a
686 speleothem from Cango Caves, Cape Province, South Africa. Quaternary Research
687 37, 203-213.

688 Tyson, P.D., Preston-Whyte, R.A., 2000. The Weather and Climate of Southern
689 Africa. Oxford University Press, Oxford.

690 van Beek, R., Cammeraat, E., Andreu, V., Mickovski, S.B., Dorren, L., 2008. Hillslope
691 processes: Mass wasting, slope stability and erosion. In: Norris, J.E., Stokes,
692 A., Mickovski, S.B., Cammeraat, E., van Beek, R., Nicoll, B.C., Achim, A. (Eds.).
693 *Slope stability and erosion control: Echotechnological solutions*. Springer, Dordrecht.

694 Whalley, W. B., 1984. Rockfalls. In: Brunnsden, D. and Prior, D. B. (Eds). *Slope*
695 *Instability*. Wiley, Chichester.

696 Williams, M., Cook, E., van der Kaars, S., Barrows, T., Shulmeister, J. and Kershaw,
697 P., 2009. Glacial and deglacial climatic patterns in Australia and surrounding regions
698 from 35 000 to 10 000 years ago reconstructed from terrestrial and near-shore proxy
699 data. *Quaternary Science Reviews* 28, 2398-2419.

700 Zurawek, R., 2003. The problem of the identification of relict rock glaciers on
701 sedimentological evidence. *Landform Analysis* 4, 7-15.

702

703 **Figure Captions**

704 **Fig. 1.** Location map showing the position of the study sites (1 = Mount Enterprise, 2
705 = Tiffindell, 3 = Killmore, 4 = Rose Hill, 5 = Carlisle's Hoek, 6 = Bokspruit, 7 =
706 Moshesh's Ford).

707

708 **Fig. 2.** Photos of the main study sites at Mount Enterprise (A), Tiffindell (B), Killmore
709 (C) and Rose Hill (D).

710

711 **Fig. 3.** Three-dimensional model of aerial imagery (A) (aerial imagery obtained from
712 the Department of Rural Development and Land Reform (0.5 m ground sample
713 distance) and then draped over 30 m ASTER DEM) and geomorphological map (B)
714 of the Mount Enterprise site showing the sample sites for surface exposure dating.
715 Sites labelled 1-3 are sedimentological descriptions, whilst features labelled A-D are
716 geomorphological landforms described in the text.

717

Fig. 4. Stratigraphic diagram showing the key sedimentological features at Mount Enterprise, Rose Hill, Carlisle's Hoek, and Moshesh's Ford.

Fig. 5. Weathering rinds observed in the lower unit of section 2 at Mount Enterprise. Note two clasts indicated by arrows that have completely weathered in situ.

Fig. 6. Three-dimensional model of aerial imagery (A) (aerial imagery obtained from the Department of Rural Development and Land Reform (0.5 m ground sample distance) and then draped over 30 m ASTER DEM) and geomorphological map (B) of the Tiffindell site showing the sample sites for surface exposure dating.

Fig. 7. Geomorphological map (A), three-dimensional model of aerial imagery (B) (aerial imagery obtained from the Department of Rural Development and Land Reform (0.5 m ground sample distance) and then draped over 30 m ASTER DEM), and block orientation (C) at the Killmore site. Box in A indicates sampling location for block orientations. Box in B indicates location of study site (A). Note the topographic control from more resistant flat-lying layers as indicated by the arrows in B.

Fig. 8. Photos illustrating the highly weathered nature of the blocks sitting on the surface of the Killmore ridge.

Fig. 9. Three-dimensional model of aerial imagery (A) (aerial imagery obtained from the Department of Rural Development and Land Reform (0.5 m ground sample distance) and then draped over 30 m ASTER DEM) and geomorphological map (B) of the Rose Hill site.

Figure 1

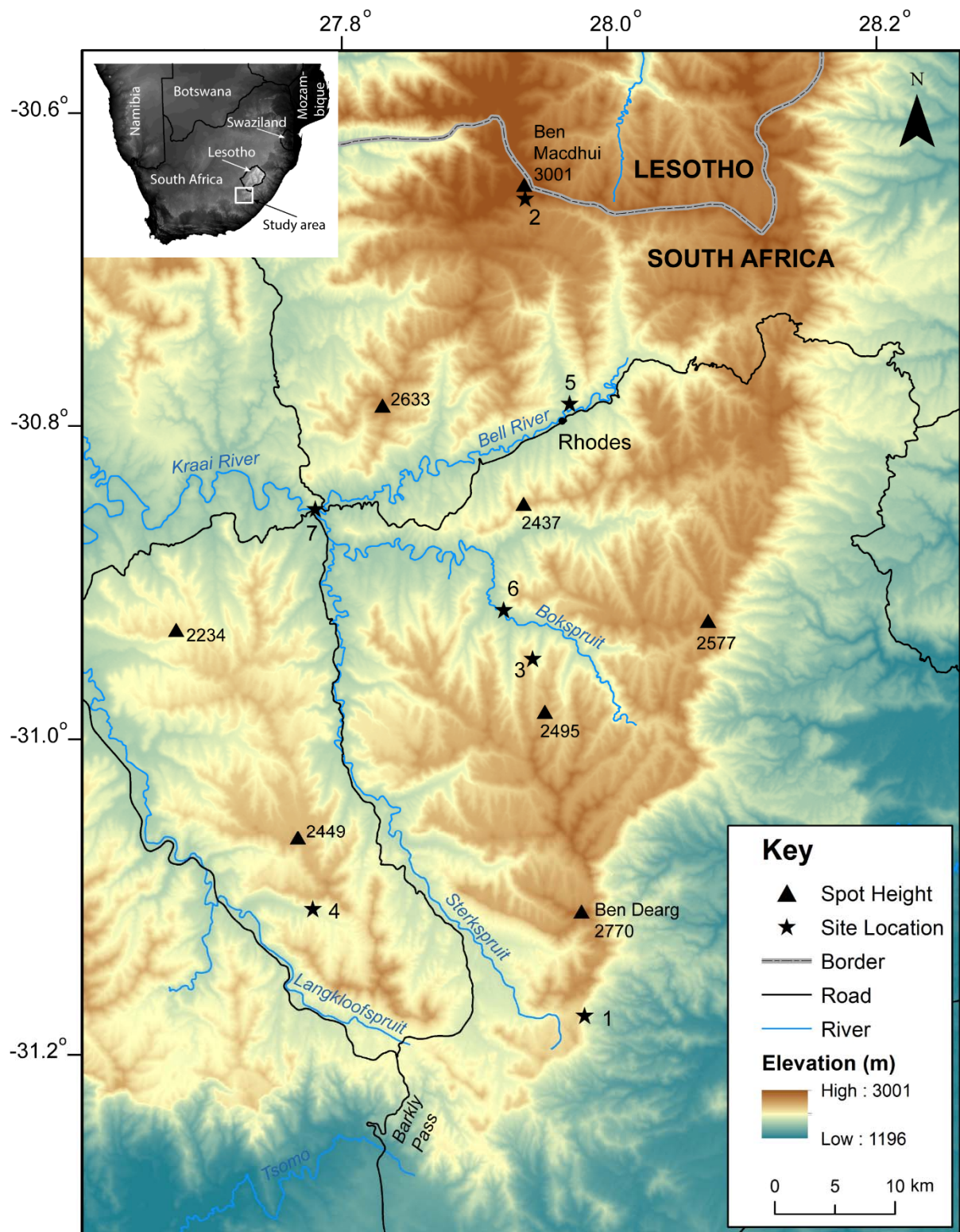


Figure 2

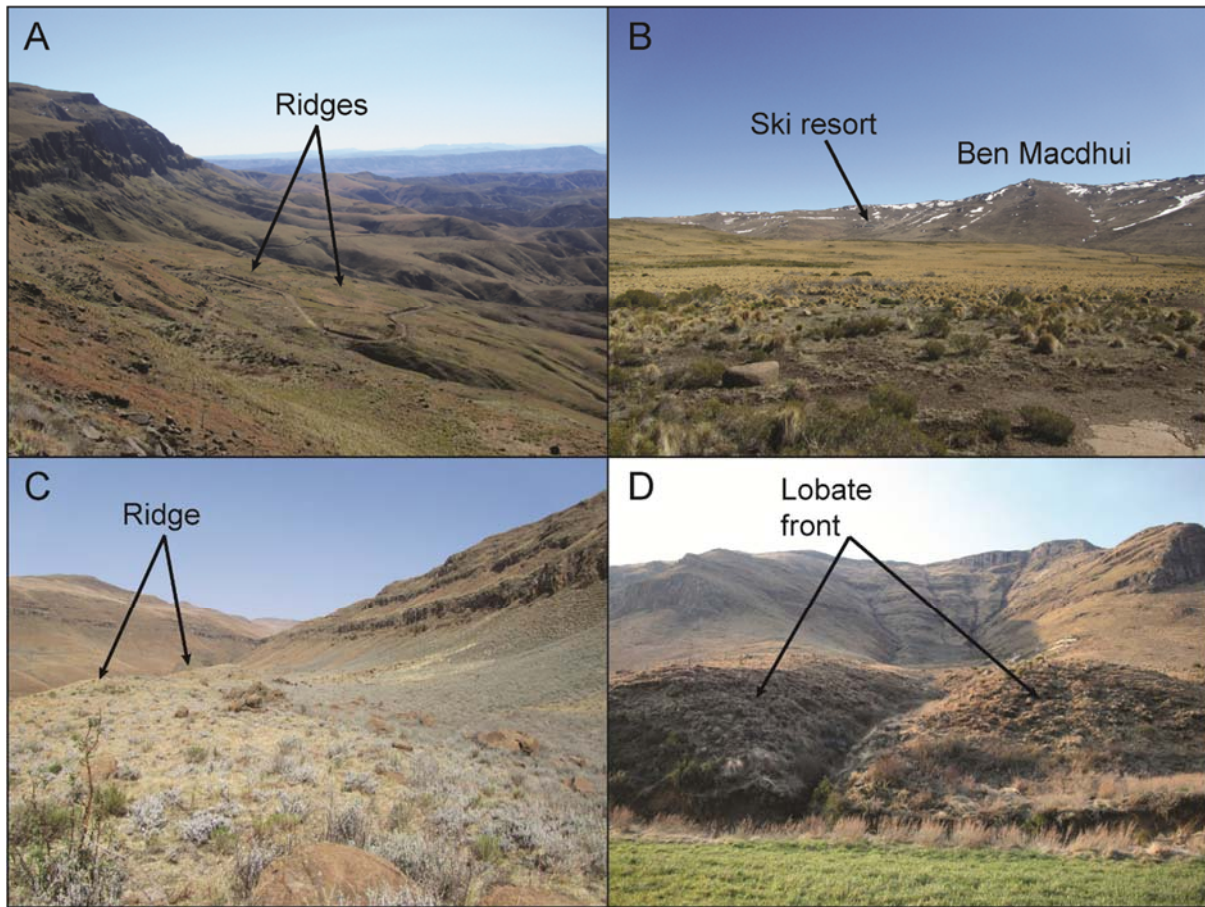


Figure 3

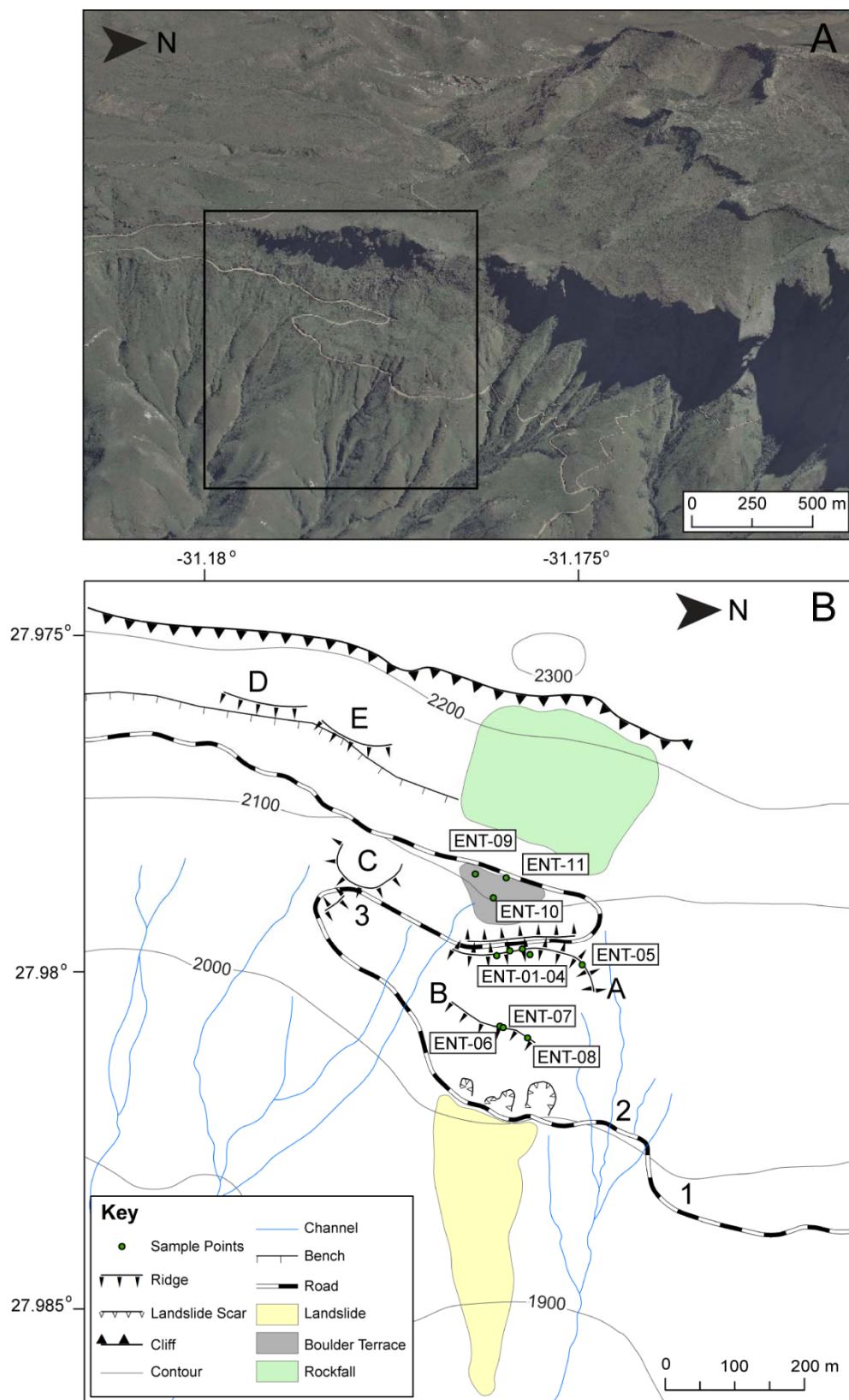


Figure 4

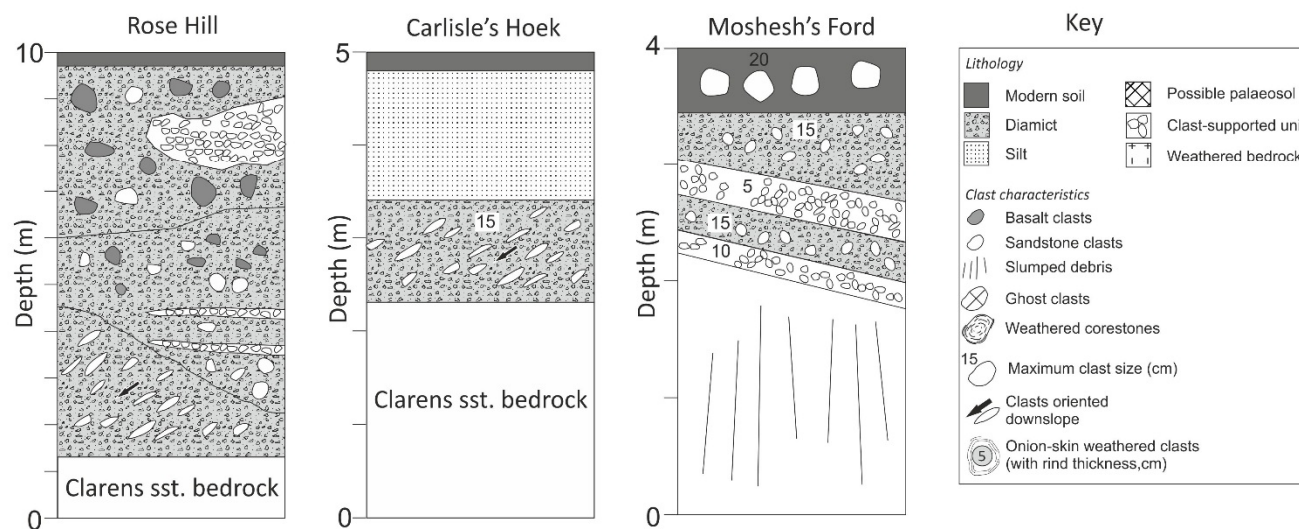
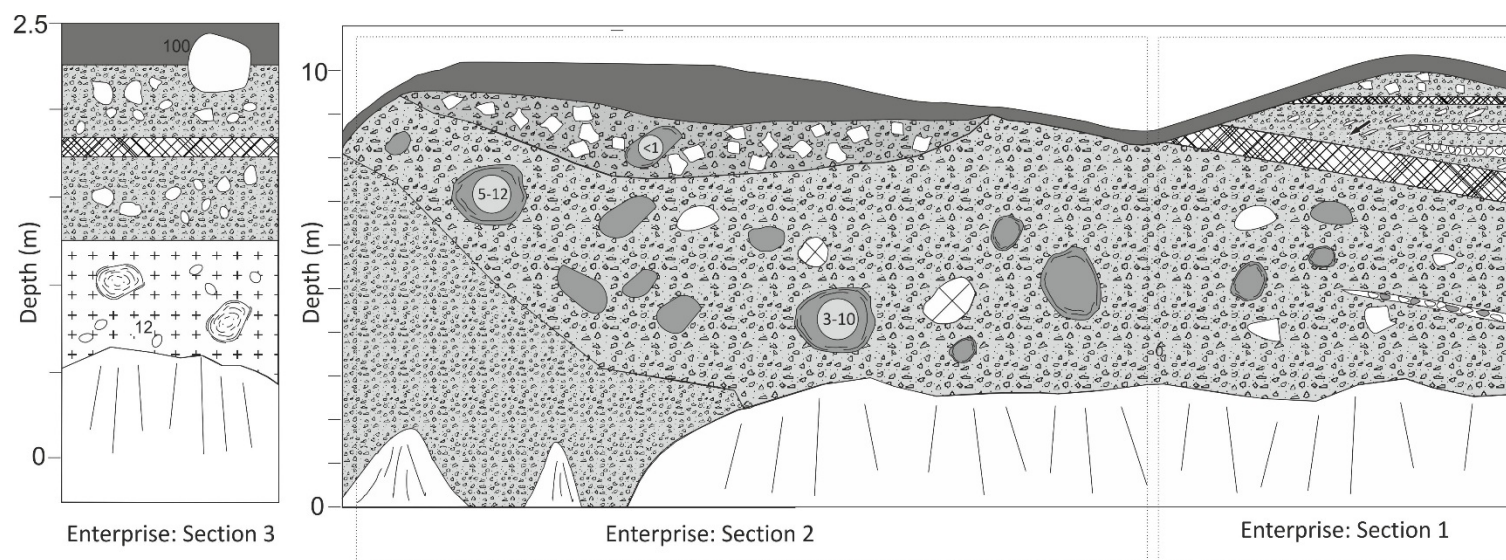


Figure 5



Figure 6

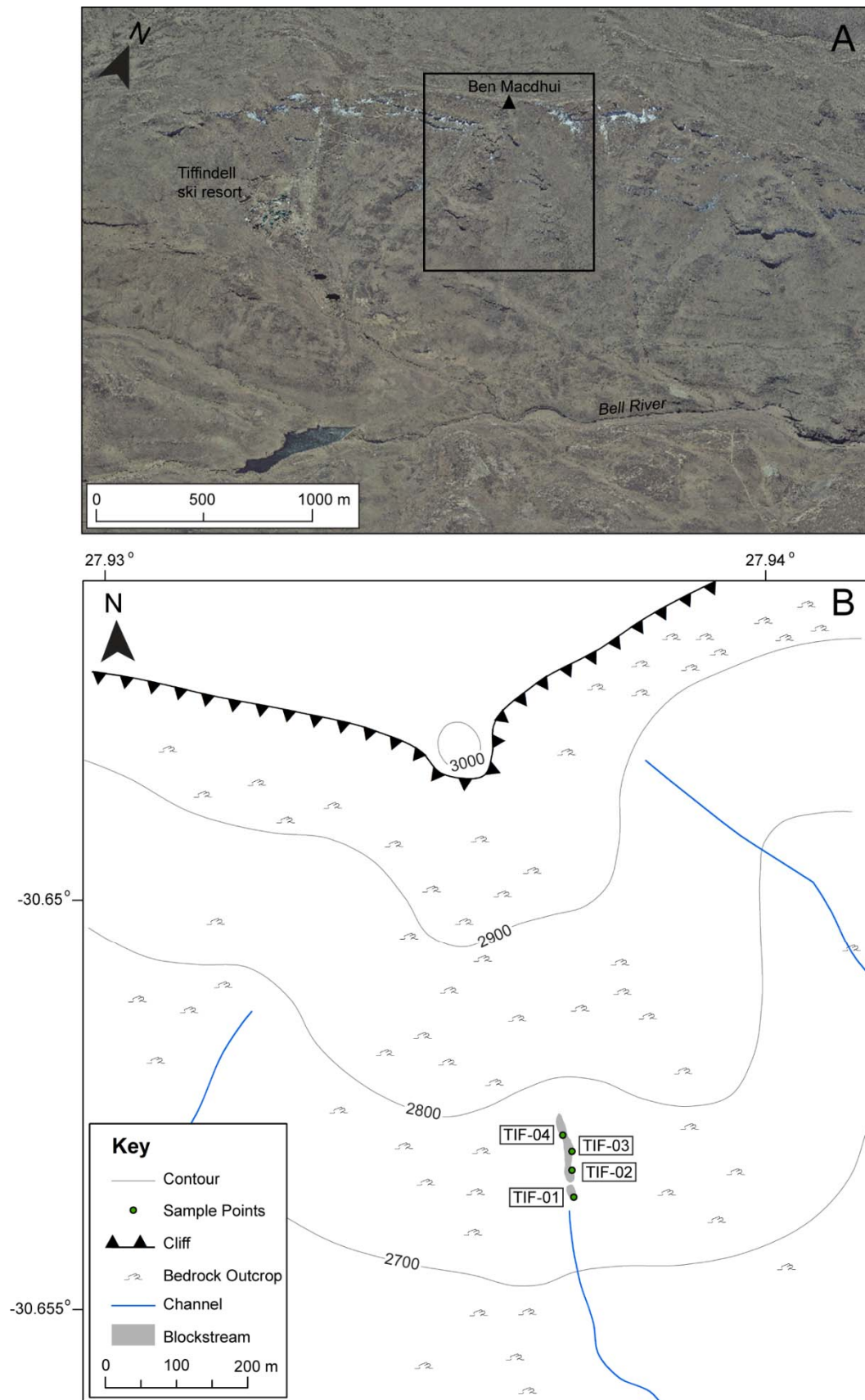


Figure 7

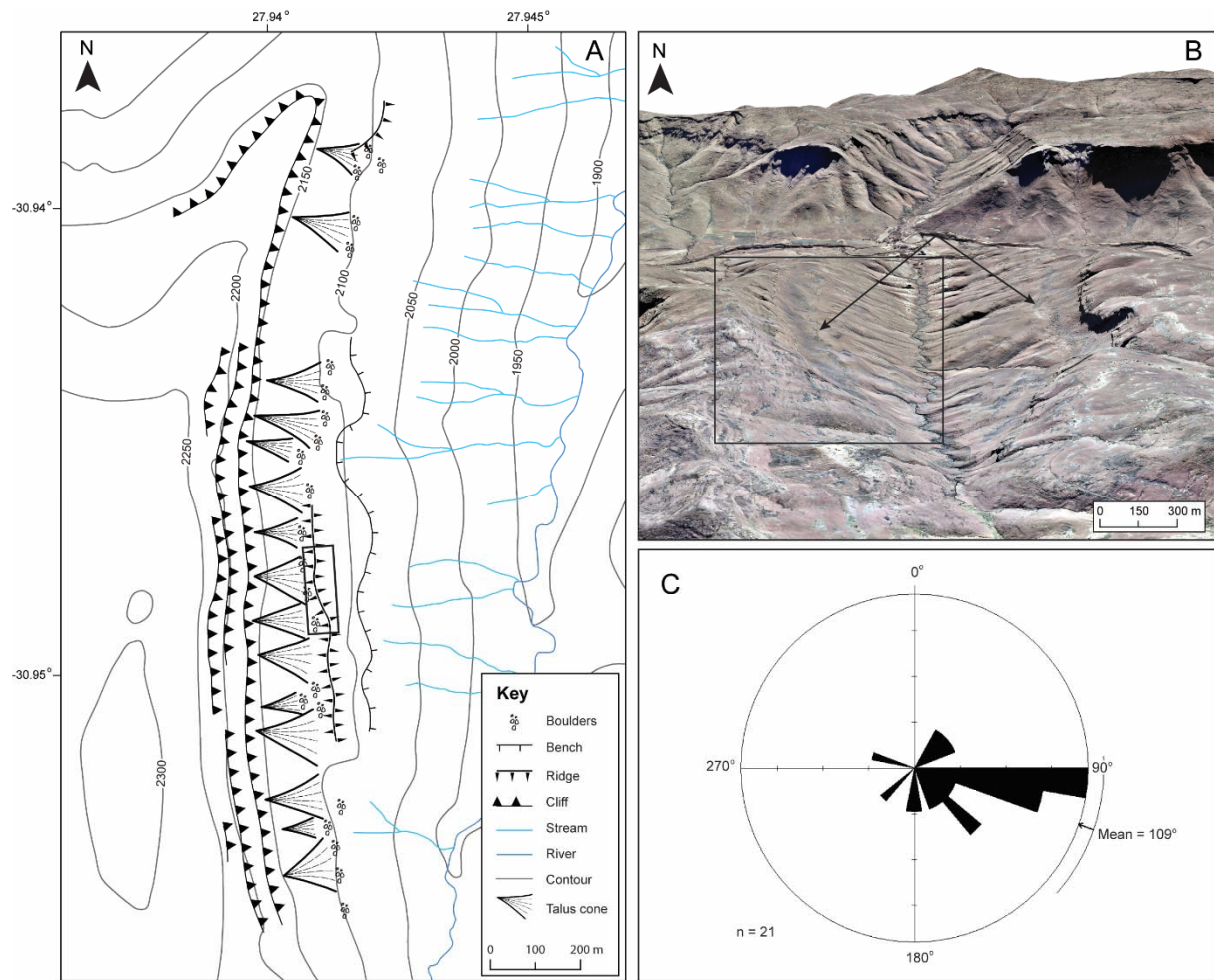


Figure 8



Figure 9

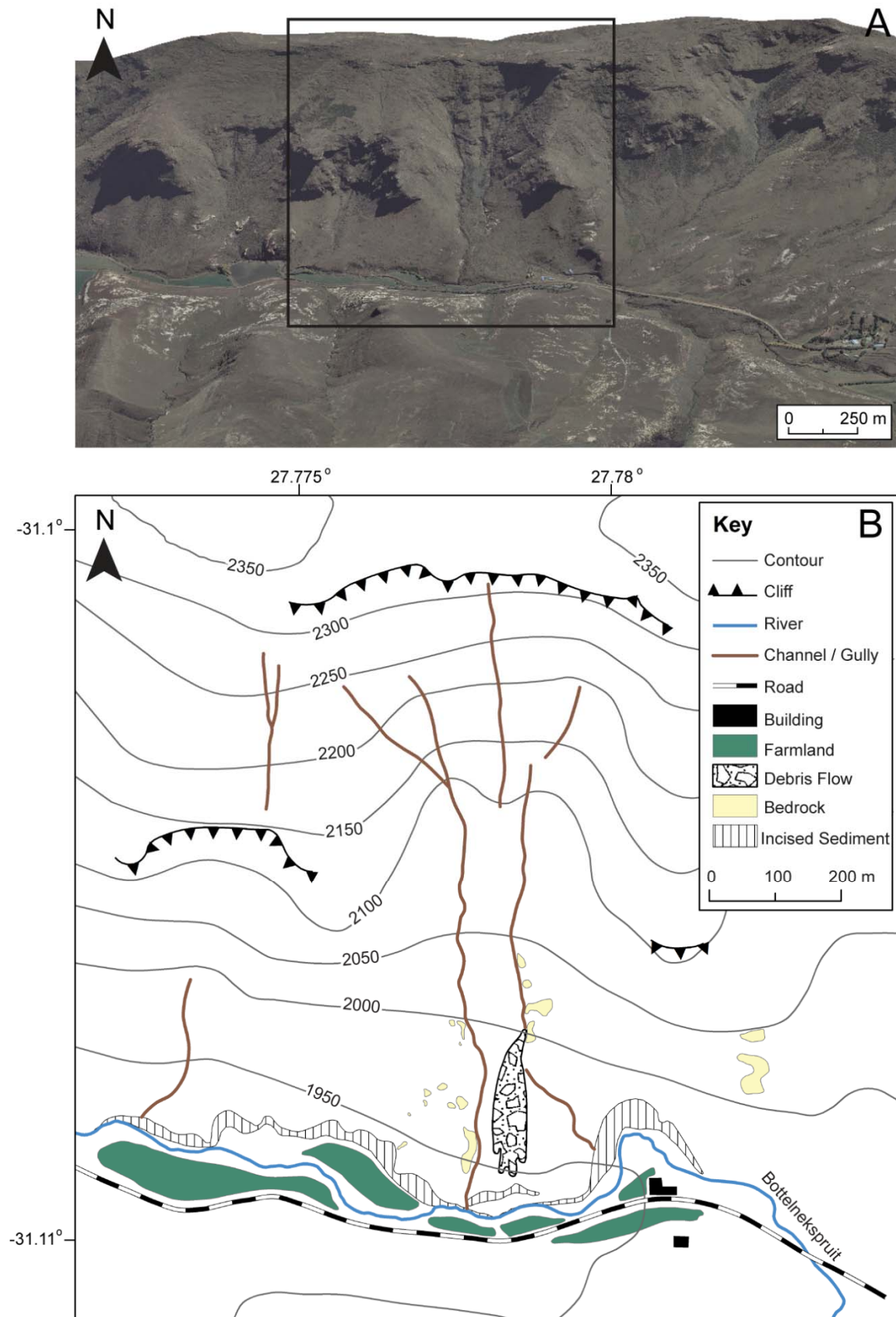


Table 1

Site information for the samples collected for surface exposure dating

Sample	Longitude (°E)	Latitude (°N)	Altitude (m) (GPS)	Altitude (m) (GIS)	Lithology ^a	Horizon correction	Thickness (cm) ^b
<i>Mount Enterprise</i>							
ENT-01	27.9798	31.1758	2087	2077	basalt	0.9864	1.8
ENT-02	27.9798	31.176	2084	2076	basalt	0.9864	2.8
ENT-03	27.9799	31.1761	2079	2068	basalt	0.9855	1.8
ENT-04	27.9799	31.1757	2073	2076	basalt	0.9854	2.9
ENT-05	27.98	31.175	2083	2075	basalt	0.9873	3.6
ENT-06	27.9809	31.1761	2052	2048	basalt	0.9902	2.4
ENT-07	27.981	31.176	2025	2048	basalt	0.9902	2.5
ENT-08	27.9811	31.1757	2044	2046	basalt	0.9905	2.0
ENT-09	27.98	31.18	2098	2100	basalt	0.9808	3.4
ENT-10	27.98	31.18	2105	2090	basalt	0.9808	4.1
ENT-11	27.98	31.18	2107	2098	basalt	0.9808	3.3
<i>Tiffindell</i>							
TIF-01	27.94	30.65	2712	2728	basalt	0.9871	2.3
TIF-02	27.94	30.65	2755	2754	basalt	0.9881	4.0
TIF-03	27.94	30.65	2772	2762	basalt	0.9854	2.6
TIF-04	27.94	30.65	2774	2775	basalt	0.9854	4.6

a. Basalt $\rho = 3.0 \text{ g.cm}^{-3}$.b. $L = 160 \text{ g.cm}^{-2}$.

Table 2³⁶Cl exposure ages for the sample sites^a

Sample	Lab code	[³⁶ Cl] _c (x10 ⁴ g ⁻¹) ^b	[³⁶ Cl] _r (x10 ² g ⁻¹) ^c	Exposure age (ka)
<i>Mount Enterprise</i>				
ENT-01	ANU-C248-21	18.65 ± 0.91	1.86 ± 0.14	10.3 ± 0.6
ENT-02	ANU-C248-22	23.83 ± 0.754	1.82 ± 0.75	9.8 ± 0.5
ENT-03	ANU-C248-23	23.57 ± 1.170	1.34 ± 0.11	12.0 ± 0.7
ENT-04	ANU-C249-09	16.94 ± 0.87	1.28 ± 0.12	9.2 ± 0.5
ENT-05	ANU-C248-24	20.04 ± 1.04	0.684 ± 0.099	11.3 ± 0.7
ENT-06	ANU-C248-25	26.79 ± 1.19	4.39 ± 0.28	11.2 ± 0.6
ENT-07	ANU-C248-26	38.02 ± 1.84	1.45 ± 0.28	20.5 ± 1.2
ENT-08	ANU-C248-27	32.56 ± 1.60	1.43 ± 0.12	17.5 ± 1.0
ENT-09	ANU-C248-28	14.29 ± 0.602	1.78 ± 0.099	7.6 ± 0.4
ENT-10	ANU-C248-29	14.93 ± 0.713	2.43 ± 0.15	7.7 ± 0.4
ENT-11	ANU-C249-11	9.332 ± 0.501	1.13 ± 0.11	5.0 ± 0.3
<i>Tiffindell</i>				
TIF-01	ANU-C249-06	127.7 ± 5.05	0.757 ± 0.064	49.3 ± 2.5
TIF-02	ANU-C249-03	39.45 ± 2.12	0.916 ± 0.063	13.6 ± 0.8
TIF-03	ANU-C249-04	77.99 ± 3.49	0.711 ± 0.060	26.1 ± 1.4
TIF-04	ANU-C249-05	38.88 ± 2.18	0.823 ± 0.056	12.7 ± 0.8

^aData are normalised to the GEC standard (³⁶Cl/Cl = 444 x 10⁻¹⁵).Carrier ³⁶Cl/Cl = 1 x 10⁻¹⁵.³⁶Cl decay constant 2.3 x 10⁻⁶ y⁻¹.

b. C = cosmogenic component.

c. R = background nucleogenic component.